Photoaffinity Labeling of Creatine Kinase with 2-Azido- and 8-Azidoadenosine Triphosphate: Identification of Two Peptides from the ATP-Binding Domain†

Michael C. Olcott,*,‡ Mary L. Bradley, and Boyd E. Haley*

College of Pharmacy and Lucille P. Markey Cancer Center, University of Kentucky, Lexington, Kentucky 40536

Received May 23, 1994; Revised Manuscript Received July 8, 1994®

ABSTRACT: Two different analogs of ATP, [γ-^{32}P]2N_3ATP and [γ-^{32}P]8N_3ATP, were used to photoaffinity label the MM and BB isoforms of rabbit cytosolic creatine kinase. Evidence that photoinsertion was within the ATP-binding domain was as follows: (1) Assays for creatine phosphate production demonstrated that [γ-^{32}]2N_3ATP and [γ-^{32}P]8N_3ATP are substrates for creatine kinase. (2) Enzymatic activity was inhibited by photolabeling with either analog. (3) Saturation of photoinsertion was observed for both analogs. Half-maximal saturation was observed at 5 μM [γ-^{32}P]2N_3ATP or 12 μM (γ-^{32}P]8N_3ATP. (4) Photoinsertion of both probes could be decreased by micromolar levels of ATP. Immobilized Al^{3+} affinity chromatography and HPLC were used to isolate the peptides modified by these probes. Overlapping sequence analysis of the isolated peptides from the tryptic and chymotryptic digests of the photolabeled MM isoform revealed that [γ-^{32}P]8N_3ATP photoinserted into the peptide region corresponding to Val^{279}–Arg^{291}, whereas [γ-^{32}P]2N_3-ATP photoinserted into Val^{236}–Lys^{241}. The corresponding peptides (Ile^{279}–Arg^{291} and Val^{236}–Lys^{241}) from the BB isoform were shown to be selectively modified. We conclude that amino acid residues within the peptide regions 236–241 and 279–291 of rabbit cytosolic creatine kinase are localized within the binding domain for the adenine moiety of ATP. The results also demonstrate the effectiveness and selectivity of Al^{3+} as the chelating agent in immobilized metal affinity chromatography for the isolation of photolabeled peptides as well as its potential to enhance retention of radiolabel during HPLC.

Creatine kinase (ATP:creatine *N*-phosphotransferase, EC 2.7.3.2) is a pivotal enzyme in high-energy phosphate metabolism that catalyzes the reversible reaction:

$$\text{creatine} + \text{ATP} \rightleftharpoons \text{creatine phosphate} + \text{ADP} + \text{H}^+$$

Found in all vertebrates, creatine kinase has the function of replenishing ATP levels in tissues with high, fluctuating energy demands such as skeletal muscle, brain, heart, and spermatozoa and is a key participant in the transfer of energy within the cell (Bessman & Carpenter, 1985; Turner et al., 1973; Wallimann et al., 1977). Two different types of subunits of cytosolic creatine kinase are known to exist in higher vertebrates: B and M. Differential expression and dimerization of these subunits account for the three isozymes found in the cytosol of various tissues. For example, skeletal muscle consists almost exclusively of the MM isoform, whereas brain expresses primarily the BB isoform. Heart tissue contains both the MM and MB isoforms. The monomeric molecular mass of both types of subunit is 43 kDa. Due to its abundance and to the differences in the relative tissue distribution of the various isozymes, creatine kinase is an important clinical tool in the diagnosis of myocardial infarction and muscular dystrophy (Harrison, 1993).

Although much is known about the kinetics and enzymology of the reaction, the three-dimensional structure of the active site of creatine kinase has not been determined. Therefore, most work has focused on identifying amino acid residues that play roles in catalysis and/or binding of substrates. Two positively charged amino acids, arginine (Borders & Riordan, 1975) and lysine (James & Cohn, 1974), have been shown to be involved and presumably provide an electrostatic attraction for the negatively charged phosphate group of the substrate. Studies using chemical modification with diethyl pyrocarbonate (Clarke & Price, 1979) and proton NMR spectroscopy (Rosevear et al., 1981) have implicated one or more histidines in the catalytic mechanism. Another approach that one can use to begin to elucidate the structure of the active site is to identify peptide regions by affinity labeling the active site with reactive substrate analogs. Marletta and Kenyon (1979) proposed that *N*-(2,3-epoxypropyl)-*N*-amidinoglycine (epoxycreatine), an analog of creatine, could be used to affinity label the creatine-binding site of creatine kinase. Subsequently, Cys^{282} was identified as the site of covalent incorporation of epoxycreatine (Buechter et al., 1992). Cys^{282} is the single highly reactive sulfhydryl of creatine kinase which is readily modified by several sulfhydryl reagents, leading to various levels of decreased enzyme activity including total inhibition (Mahowald et al., 1962; O'Sullivan & Cohn, 1966). However, Furter et al. (1993) recently demonstrated that the homologous reactive cysteine in the chicken cardiac mitochondrial enzyme is required for synergism but is nonessential for catalysis.

To further characterize the active site of creatine kinase, we have used two azidopurine analogs of the other substrate, ATP, in the present study to photoaffinity label the MM and BB isoforms. Since photoinsertion of the 2-azido- and 8-azidoadenine nucleotide analogs can occur at different amino acid residues due to the positioning of the azide moiety on opposite ends of the purine ring, they present an attractive opportunity to identify two distinct regions within the adenine-binding domain of ATP-binding proteins such as creatine kinase.

† This work was supported by National Institutes of Health Grant GM35766 and by funds from the Lexington Clinic Foundation.

* Authors to whom correspondence should be addressed.

‡ Present address: Department of Molecular Biology, Stockholm University, S-106 91 Stockholm, Sweden. Telephone: 46-8-164188. Fax: 46-8-152350.

® Abstract published in *Advance ACS Abstracts,* September 1, 1994.

0006-2960/94/0433-11935$04.50/0

Previous work by Andersson and Porath (1986) and others described the use of immobilized Fe^{3+} affinity chromatography to isolate phosphorylated peptides or proteins (Muszynska et al., 1986; Murakami et al., 1990). Subsequently, our laboratory has used a modification of this technique to isolate and identify specific nucleotide-binding site peptides from photolabeled adenylate kinase (Salvucci et al., 1992), botulinum C3 ADP-ribosyltransferase (Chavan et al., 1992), glutamate dehydrogenase (Shoemaker & Haley, 1993), and prostaglandin dehydrogenase (Chavan et al., 1993). In the present study, we have used an improved type of immobilized metal affinity chromatography to isolate peptides from creatine kinase photolabeled by the two different azido analogs of ATP. A preliminary account of some of these data has been previously reported (Olcott & Haley, 1993).

MATERIALS AND METHODS

Materials. Rabbit creatine kinase from skeletal muscle, heart, and brain was obtained from Sigma Chemical Co. (St. Louis, MO). [γ-^{32}P]$8N_3$ATP[1] was synthesized and purified as previously described (Potter & Haley, 1983). [γ-^{32}P]$2N_3$-ATP was synthesized from $2N_3$ATP by the same exchange reaction as described by Potter and Haley (1983). $2N_3$ATP was synthesized from $2N_3$AMP by the coupling procedure of Michelson (1964). $2N_3$AMP was prepared as described by Kim and Haley (1990). Sequencing grade modified trypsin was from Promega Biotec.

Photoaffinity Labeling and SDS–PAGE. One to four micrograms of creatine kinase was incubated with photoprobe at the appropriate concentration in 60 μL of 50 mM Tris-HCl or 10 mM NaH_2PO_4 containing $MgCl_2$ and creatine at the concentrations and pH described in the figure legends. The reaction was initiated by the addition of photoprobe. After a 30-s incubation at 4 °C, the solution was photolyzed for 30–90 s with a 254-nm UV lamp (3800 μW/cm^2 at 4 cm). The reaction was stopped by the addition of a protein-solubilizing mixture containing 60 mM Tris-HCl (pH 9.0), 2.5% SDS, 75% sucrose, 200 mM dithiothreitol, and pyronin Y. After solubilization, the samples were subjected to electrophoresis in a 10% acrylamide separating gel with a 4% acrylamide stacking gel according to the method of Laemmli (1970). Quantification of ^{32}P incorporation was accomplished by scintillation counting of the excised labeled bands from the dried gel and by analysis with an Ambis 4000 Imaging System.

Quantification of Creatine Phosphate Production by TLC. Approximately 0.2 μL of the reaction mixture was spotted on PEI–cellulose F and developed in 0.3 M ammonium bicarbonate. R_f values for [γ-^{32}P]ATP, [γ-^{32}P]$2N_3$ATP, [γ-^{32}P]-$8N_3$ATP, and creatine phosphate were 0.13, 0.08, 0.11, and 0.95, respectively. The percentage of ^{32}P migrating as creatine phosphate was determined by analyzing the TLC plate with an Ambis 4000 Imaging System. The number of picomoles of creatine phosphate produced was calculated by multiplying this percentage by 6000 (picomoles of nucleotide substrate before reaction initiation).

Determination of Stoichiometry. Photolabeled creatine kinase was precipitated with 0.5 mL of ice-cold 8% trichloroacetic acid containing 1.0 mM ATP and microfuged for 5 min at 4 °C. The pellet was rinsed with 200 μL of ice-cold methanol, resuspended in 100 μL of a solubilizing mix containing 2 M urea and 7.5 mM potassium phosphate, pH 7.4, and then counted by liquid scintillation.

Photoaffinity Labeling and Proteolysis for Peptide Isolation. Photoaffinity labeling was conducted at 4 °C in 725 μL reaction mixtures containing 10 mM NaH_2PO_4, pH 7.0, 5 mM creatine, 1 mM $MgCl_2$, and the appropriate concentration of photoprobe. The reaction was initiated by the addition of photoprobe. After a 60-s incubation, the solution was photolyzed for 30 s. This procedure was repeated following the addition of a second dose of photoprobe. The reaction was terminated by the addition of 500 μL of ice-cold 20% perchloric acid. After removal of the supernatant, the precipitate was washed with methanol and then resolubilized with 600 μL of 1% ammonium acetate/1.2 M urea, pH 7.9. The resolubilized protein was then incubated with either 600 μg of chymotrypsin or 20 μg of sequencing grade modified trypsin at room temperature for 24 h.

Immobilized Al^{3+} Affinity Chromatography. Two milliliters of iminodiacetic acid epoxy-activated Sepharose 6B resin was prepared for affinity chromatography by washing successively with 20 mL of H_2O, 10 mL of 50 mM $AlCl_3$, and 20 mL of H_2O and then equilibrated with 20 mL of 1% ammonium acetate/1 M NaCl, pH 5.8 (buffer A). The solution containing digested photolabeled protein was acidified to pH 6 and then loaded on the immobilized Al^{3+} column. After the column was washed with 10 mL of buffer A, the photolabeled peptides were eluted with 10 mL of 10 mM K_2HPO_4, pH 7.4 (buffer B). During chromatography, 2.0-mL fractions were collected, and radioactivity was determined by liquid scintillation.

Reverse Phase HPLC. The photolabeled peptides were separated on an Aquapore RP-300 C8 column (250 × 4.6 mm) using the following gradient: 0% solvent B at 0 min, 0% solvent B at 10 min, 30% solvent B at 20 min, 60% solvent B at 60 min, and 100% solvent B at 70 min (solvent A, 0.1% trifluoroacetic acid/50 μM $AlCl_3$; solvent B, 80% acetonitrile/0.1% trifluoroacetic acid). The flow rate for the entire gradient was 0.5 mL/min. Fractions containing significant radioactivity with a corresponding absorbance at 210 nm were analyzed on an Applied Biosystems 477A protein sequencer.

RESULTS

Preliminary studies demonstrated that [γ-^{32}P]$8N_3$ATP could be used to photolabel creatine kinase isolated from rabbit skeletal muscle (MM), heart muscle (MM as purified by Sigma), and brain (BB). Because of the complexity of the photolabeled bands observed in the skeletal muscle preparation (data not shown), the heart muscle and brain preparations were used as sources for the MM and BB isoforms, respectively.

To optimize conditions for photolabeling creatine kinase, the effects of pH and time of photolysis were examined. Using 10 mM NaH_2PO_4 as the buffer for reaction mixtures of varying pH (5–9), we determined that optimal photolabeling of either isoform with [γ-^{32}P]$8N_3$ATP occurs at pH 6.5 (data not shown). Because the substrate properties of [γ-^{32}P]$2N_3$ATP and [γ-^{32}P]$8N_3$ATP were determined at pH 7.0 and the photolabeling observed at pH 7.0 was nearly as effective as that observed at pH 6.5, most of the remaining experiments were done at pH 7.0. Maximum photoinsertion of either probe was achieved after approximately 90 s of UV irradiation. No significant labeling was observed when a sample was incubated in the absence of UV light (data not shown).

To demonstrate that the 2-azido and 8-azido analogs of ATP interact with the active site of creatine kinase, the ability of [γ-^{32}P]$2N_3$ATP and [γ-^{32}P]$8N_3$ATP to serve as substrates for creatine kinase was examined. Figure 1 shows the results

[1] Abbreviations: $8N_3$ATP, 8-azidoadenosine 5′-triphosphate; $2N_3$-ATP, 2-azidoadenosine 5′-triphosphate; HPLC, high-performance liquid chromatography; TLC, thin-layer chromatography; SDS–PAGE, sodium dodecyl sulfate–polyacrylamide gel electrophoresis; PEI, poly(ethylenimine).

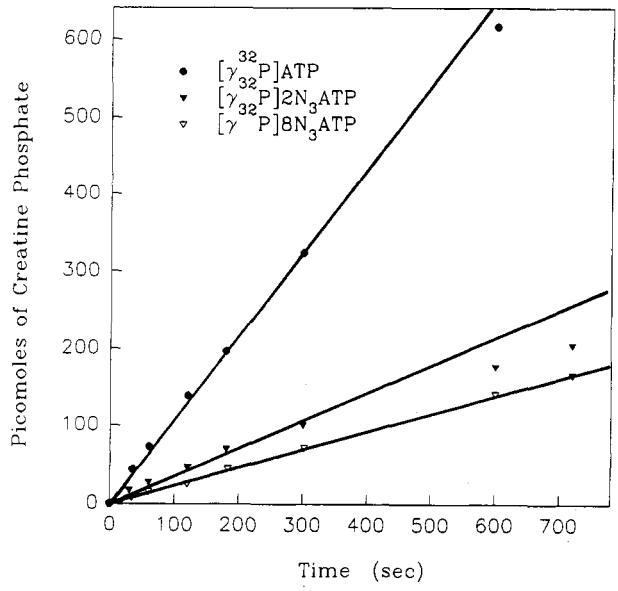

FIGURE 1: [γ-^{32}P]2N_3ATP and [γ-^{32}P]8N_3ATP as substrates for creatine kinase. 0.2 μg of heart creatine kinase was incubated in a 60-μL reaction mixture containing 10 mM NaH_2PO_4, pH 7.0, 5 mM creatine, 1 mM $MgCl_2$, 1 mM β-mercaptoethanol, and 100 μM of either [γ-^{32}P]ATP, [γ-^{32}P]2N_3ATP, or [γ-^{32}P]8N_3ATP. After incubating at 22 °C for the appropriate time, creatine phosphate production was determined by thin-layer chromatography and radioanalytic imaging as described under Materials and Methods.

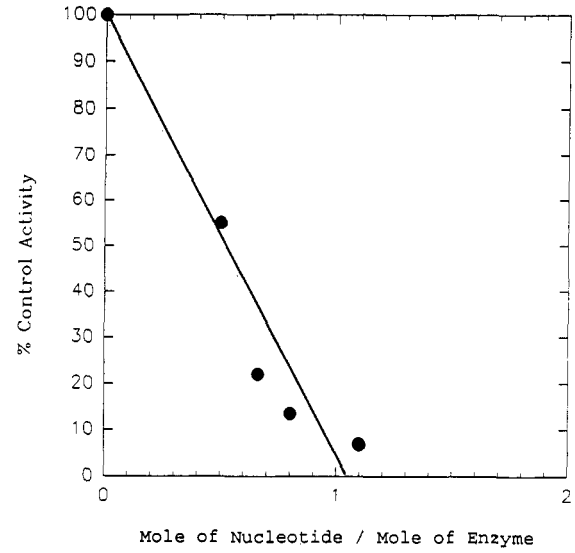

FIGURE 2: Effect of photolabeling on creatine kinase activity. 1.0 μg of rabbit heart creatine kinase was incubated in a 60-μL reaction mixture containing 10 mM Tris, pH 7.0, 1 mM $MgCl_2$, and various concentrations of [γ-^{32}P]2N_3ATP. Following a 30-s incubation at 4 °C, the samples were irradiated as described under Materials and Methods. Enzymatic activity was determined by a colorimetric assay (Sigma diagnostic kit 661), and the stoichiometry was determined as described under Materials and Methods.

from an experiment in which the rate of creatine phosphate production was determined at 22 °C using [γ-^{32}P]ATP, [γ-^{32}P]2N_3ATP, and [γ-^{32}P]8N_3ATP as substrates. Both analogs were used as substrates by creatine kinase as demonstrated by the time-dependent transfer of their radiolabeled γ-phosphate to creatine. Under these conditions, the reaction rate was constant for at least 4 min when using any one of the three substrates. The loss of linearity observed after 300 s when using [γ-^{32}P]2N_3ATP as a substrate may be due to the time-dependent formation of the tetrazole form of the purine ring. Initial reaction rates (indicated by the lines) for [γ-^{32}P]ATP, [γ-^{32}P]2N_3ATP, and [γ-^{32}P]8N_3ATP were 0.32, 0.11, and 0.07 μmol min^{-1} mg^{-1}, respectively. In a separate experiment that used 1.0 μg of creatine kinase in each reaction under identical conditions as described in Figure 1, it was observed that 4.1% of [γ-^{32}P]ATP, 1.4% of [γ-^{32}P]2N_3ATP, and 1.0% of [γ-^{32}P]8N_3ATP were converted to creatine phosphate after 30 s at 22 °C. When the reaction temperature was lowered to 4 °C, these values dropped to 2.1, 0.7, and 0.6%, respectively. Creatine phosphate production was not detected when β-mercaptoethanol was excluded from the reaction mixture. Using a colorimetric assay (Sigma diagnostic kit no. 661) for the production of creatine phosphate, we confirmed that 2N_3ATP and 8N_3ATP are substrates for the MM and BB isoforms of creatine kinase (data not shown).

Figure 2 demonstrates the effect of photolabeling heart creatine kinase with [γ-^{32}P]2N_3ATP on enzymatic activity. As shown, there was a linear correlation between moles of probe incorporated and loss of enzymatic activity. The results indicate that incorporation of approximately 1 mol of probe per mole of enzyme is required to achieve 100% inhibition of activity. From control samples in these enzyme inhibition studies, it was observed that 25 and 50 μM prephotolyzed 2N_3ATP inhibited the activity by 17 and 29%, respectively, whereas 5 and 10 μM had no detectable effect. These results indicate that the photoproduct of 2N_3ATP may have an affinity for the active site.

To confirm that photoinsertion of probe is occurring within the active site, it is also necessary to demonstrate that

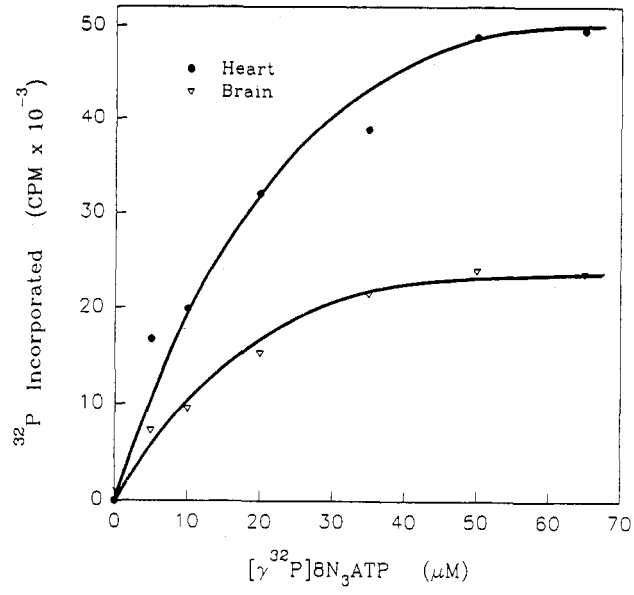

FIGURE 3: Saturation of [γ-^{32}P]8N_3ATP photoincorporation into the MM and BB isoforms of creatine kinase. 1.0 μg of creatine kinase from either heart or brain was incubated with increasing concentrations of [γ-^{32}P]8N_3ATP in 10 mM NaH_2PO_4, pH 7.0, 5 mM creatine, and 1 mM $MgCl_2$. After a 30-s incubation, the samples were irradiated for 90 s, subjected to SDS–PAGE, and then analyzed as described under Materials and Methods.

photolabeling is both saturable and able to be protected by the natural nucleotide. Figure 3 depicts the results from an experiment in which the MM and BB isoforms of creatine kinase were photolabeled with increasing concentrations of [γ-^{32}P]8N_3ATP. Both isoforms exhibited saturation at 50 μM and displayed half-maximal saturation at approximately 12 μM 8N_3ATP. In Figure 4, the MM isoform was photolabeled with increasing concentrations of [γ-^{32}P]2N_3-ATP in either the presence or the absence of 5 mM creatine. In both cases, saturation was observed near 15 μM (half-maximal saturation of 5 μM). An identical curve that yielded the same values was observed for the BB isoform (data not shown). Thus, both the MM and BB isoforms have a higher

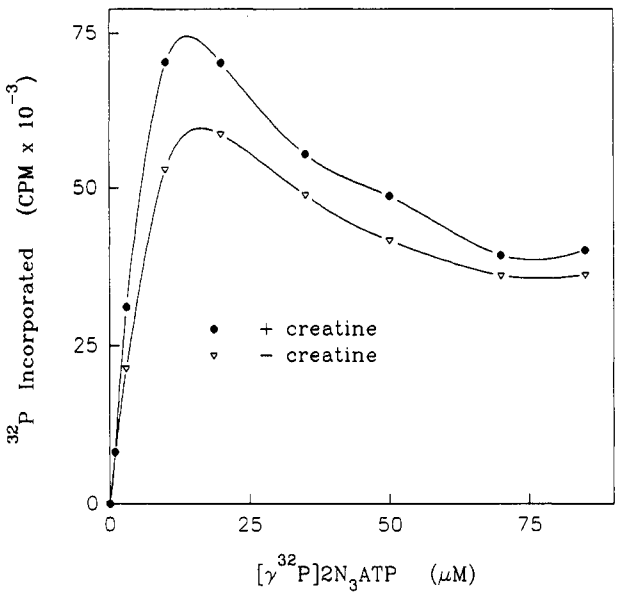

FIGURE 4: Saturation of [γ-^{32}P]2N$_3$ATP photoincorporation into the MM isoform of creatine kinase. 1.0 μg of creatine kinase from heart was incubated with increasing concentrations of [γ-^{32}P]2N$_3$-ATP in 60-μL solutions containing 10 mM NaH_2PO_4, pH 7.0, and 1 mM $MgCl_2$ in either the presence or the absence of 5 mM creatine. After a 30-s incubation, the samples were irradiated for 90 s, subjected to SDS–PAGE, and then analyzed as described under Materials and Methods.

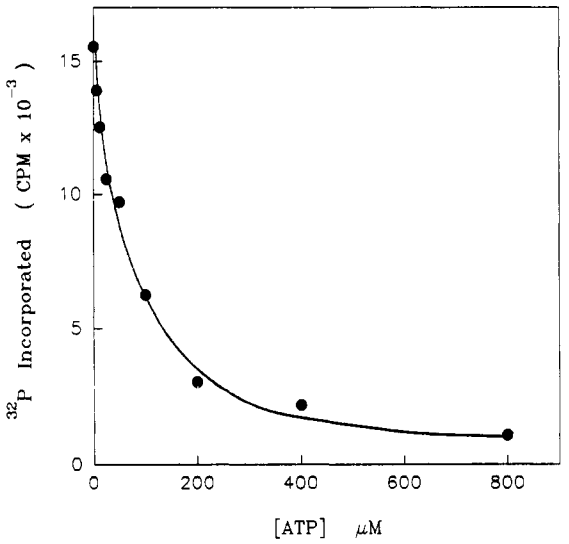

FIGURE 5: ATP protection against [γ-^{32}P]8N$_3$ATP photoincorporation into the MM isoform of creatine kinase. 1.0 μg of creatine kinase from heart muscle was incubated in 60-μL solutions containing 50 mM Tris-HCl, pH 8.0, 50 μM [γ-^{32}P]8N$_3$ATP, 10 mM creatine, 1mM $MgCl_2$, and increasing concentrations of ATP. After a 15-s incubation, the samples were irradiated, subjected to SDS–PAGE, and then analyzed as described under Materials and Methods.

affinity for the 2-azido analog than the 8-azido analog. These data are consistent with the kinetic data from Figure 1. The cause of the decrease in photoincorporation of [γ-^{32}P]2N$_3$-ATP at concentrations above 15 μM was unclear (see Discussion). In a separate set of experiments, using the procedure for determining stoichiometry from Figure 2, it was determined that 0.9–1.0 and 0.8–0.9 mol of nucleotide was incorporated per mole of enzyme when photolyzed in the presence of saturating concentrations of [γ-^{32}P]2N$_3$ATP (15 μM) and [γ-^{32}P]8N$_3$ATP (50 μM), respectively.

The ability of ATP to inhibit the photoinsertion of its 8-azido analog is shown in Figure 5; 75 μM ATP decreased photoinsertion of 50 μM [α-^{32}P]8N$_3$ATP into the MM isoform by 50%, whereas 400 μM ATP caused an 86% decrease. Similar protection against [γ-^{32}P]2N$_2$ATP photoinsertion by ATP was also observed (data not shown). In another experiment that examined the specificity of nucleotide interaction with creatine kinase, 100 μM ATP, AMP, adenine, and GTP decreased photoinsertion of 50 μM [γ-^{32}P]8N$_3$ATP by 60, 26, 24, and 21%, respectively.

Initial studies using immobilized Fe^{3+} affinity chromatography to isolate photolabeled peptides from creatine kinase were complicated by the retention of a relatively large amount of nonmodified, carboxylic acid-rich peptides by the immobilized Fe^{3+} column and the apparent contamination of the photolabeled peptide fractions upon subsequent HPLC. In experiments that utilized trypsin as the protease, the peptide S^{15}EEEYPDLSK eluted near and overlapped with the peptide that was subsequently shown to be the major photolabeled peptide. Another peptide, G^{116}GDDLDPHYVLSSR, was also prevalent. Two observations suggested that these two carboxylic acid-rich peptides were nonphotolabeled peptides: (1) the A_{210} and ^{32}P profiles never comigrated to the degree expected. (2) The same peptides also appeared in a control experiment in which nonphotolabeled creatine kinase was subjected to the identical treatment and analysis (data not shown).

Concerned that the retention of these two peptides by the immobilized Fe^{3+} column was due to an interaction of the Fe^{3+} with the carboxylic acid groups rather than the phosphate group of photolabeled peptides, we investigated the ability of immobilized Al^{3+} to act more selectively for phosphate. As shown below, these initial studies were successful in that neither of these carboxylic acid-rich peptides was retained by the immobilized Al^{3+} column. Yet more than 98% of the radiolabeled peptides was retained. Also, it appeared that more radiolabel was eluting in the fractions containing photolabeled peptide upon subsequent HPLC as compared to HPLC of peptides eluted from the immobilized Fe^{3+} column.

This latter observation prompted a study to examine the effects of various metal ions on the retention of radiolabel during reverse phase HPLC of photolabeled peptides. Creatine kinase was photolabeled with [γ-^{32}P]8N$_3$ATP, digested with chymotrypsin, and then divided into four aliquots to which either H_2O, $MnCl_2$, $FeCl_3$, or $AlCl_3$ was added, giving a final metal ion concentration of 100 μM. Each aliquot was then subjected to HPLC according to the protocol described under Materials and Methods, except that solvent A consisted of only 0.1% trifluoroacetic acid. The absorbance profiles from the four runs were virtually identical. Radioactivity profiles revealed no qualitative differences but did exhibit significant quantitative differences. The radioactivity (cpm × 10^{-3}) contained in the major peptide fraction from each of the four runs was as follows: control (no metal added), 455; Mn^{2+}, 487; Fe^{3+}, 590; Al^{3+}, 663. In an identical study using 3-phosphoglycerate kinase, retention of radiolabel in the presence of 100 μM $AlCl_3$ was increased more than 3-fold over that of the control whereas Mn^{2+} and Fe^{3+} demonstrated no significant difference from the control (data not shown). The inclusion of 50 μM $AlCl_3$ in solvent A in subsequent experiments with creatine kinase further improved retention of photoinserted label.

Figure 6 shows the radioactivity profile of immobilized Al^{3+} affinity chromatography of a chymotryptic digest of rabbit heart creatine kinase photolabeled with [γ-^{32}P]8N$_3$ATP. Over 75% of the radioactivity was recovered in the 10 mL of phosphate elution buffer, whereas less than 2% was lost in the wash fractions. Further experiments revealed that the remaining counts could be eluted by continuing the elution

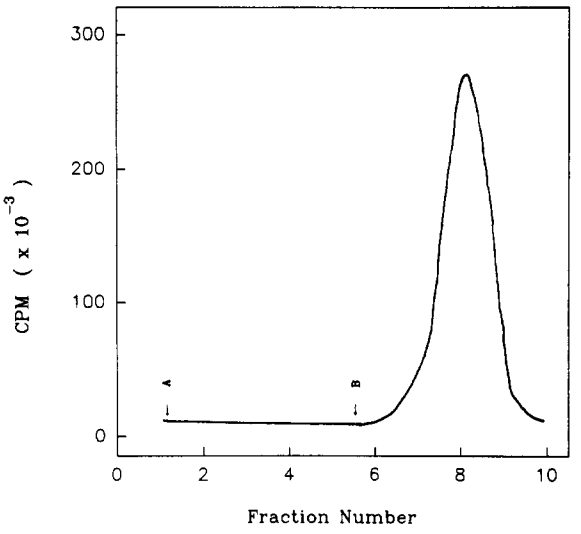

FIGURE 6: Immobilized Al^{3+} affinity chromatography of chymotrypsin-digested heart creatine kinase photolabeled with [γ-^{32}P]8N_3-ATP. 500 μg of rabbit heart creatine kinase was photolabeled with 50 μM [γ-^{32}P]8N_3ATP and digested with chymotrypsin as described under Materials and Methods. The digested material was then loaded on an immobilized Al^{3+} column equilibrated with 1% ammonium acetate/1.0 M NaCl, pH 4.8 (buffer A), and washed with 10 mL of buffer A while collecting 2-mL fractions. The photolabeled peptides were eluted with 10 mM K_2HPO_4, pH 7.4 (buffer B), and counted by liquid scintillation.

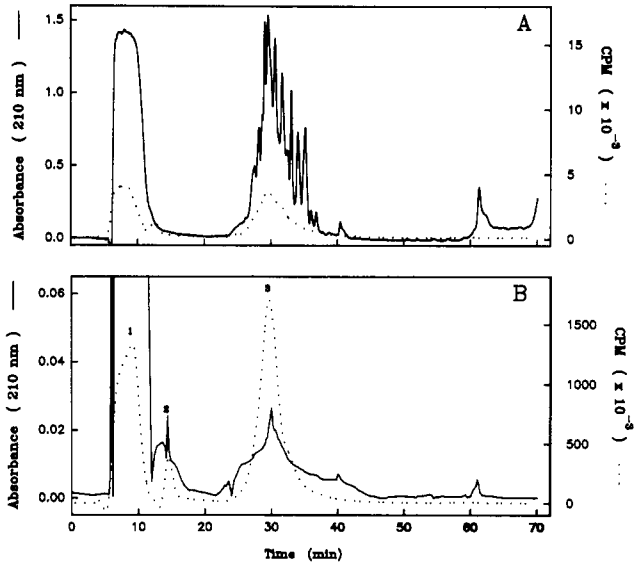

FIGURE 7: Reverse phase HPLC. The parameters for analysis were as described under Materials and Methods. To maximize retention of radiolabel, a flow rate of 0.5 mL/min was utilized, and 50 μM $AlCl_3$ was included in solvent A. (A) Analysis of fraction 2 from Figure 6. (B) Analysis of pooled fractions 6–10 from Figure 6.

and that these slower eluting peptides display the same absorbance profile on subsequent HPLC analysis.

A flow-through fraction from the immobilized Al^{3+} column (fraction 2 in Figure 6) was analyzed by HPLC. The results, shown in Figure 7A, indicate the presence of high levels of numerous peptides but low levels of radiolabel. In contrast, when fractions 6–10 (10 mL total) from Figure 6 were pooled, concentrated, and analyzed by HPLC, the results revealed only three radioactive peaks (Figure 7B). The first two radioactive peaks were always seen, even in control experiments in which only photolyzed probe was analyzed. No peptides were ever detected in either of these two peaks. The third radioactive peak contained over 1.8×10^{-6} cpm. Amino acid sequence analysis of this fraction revealed only one peptide, with a sequence corresponding to V^{279}LTCPSNLGTGLR

Table 1: Amino Acid Sequence Analysis of Radiolabeled Peptides of Rabbit Creatine Kinase Photolabeled with [γ-^{32}P]8N_3ATP

amino acid (pmol)		
heart		brain
trypsin	chymotrypsin	chymotrypsin
A (32)		
G (35)		
H (3)		
P (20)		
F (22)		
M (17)		
W (11)		
N (11)		
E (9)		
H (ND)[a]		
L (18)		
G (12)		
Y (7)		
V (10)	V (61)	I (14)
L (13)	L (57)	L (43)
T (6)	T (31)	T (28)
C (ND)	C (ND)	C (ND)
P (6)	P (32)	P (46)
S (3)	S (11)	S (18)
N (4)	N (23)	N (11)
L (7)	L (6)	L (8)
G (8)	G (9)	G (22)
T (5)	T (2)	T (15)
G (9)	G (7)	G (17)
L (16)	L (ND)	L (4)
R (ND)	R (ND)	R (2)

[a] ND indicates not detected.

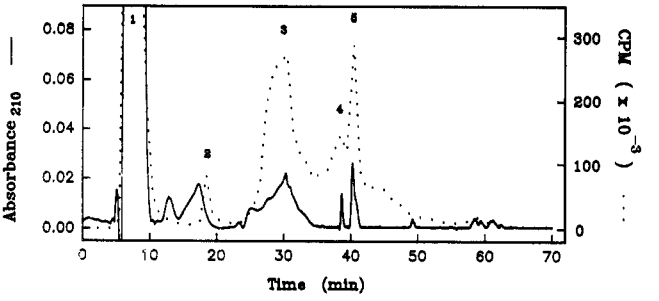

FIGURE 8: Reverse phase HPLC of immobilized Al^{3+}-purified tryptic peptides of heart creatine kinase photolabeled with [γ-^{32}P]8N_3ATP. 500 μg of rabbit heart creatine kinase was photolabeled with 50 μM [γ-^{32}P]8N_3ATP and digested with trypsin as described under Materials and Methods. After purification by immobilized Al^{3+} affinity chromatography, the photolabeled peptides were injected into a reverse phase C8 column and eluted as described under Materials and Methods.

(Table 1). An HPLC profile identical to the one in Figure 7B was oberved when [α-^{32}P]8N_3ATP was used as the photoaffinity probe, and the same peptide was revealed upon sequencing (data not shown).

To confirm the chymotryptic peptide data, photolabeled heart creatine kinase was digested with trypsin and purified by immobilized Al^{3+} affinity chromatography. The ^{32}P-containing fractions were again pooled, dried, and analyzed by HPLC as shown in Figure 8. Five major radioactive peaks were detected. Again, peaks 1 and 2 contained no detectable peptides upon sequencing. Sequence analysis of peaks 3–5 yielded the following results: peak 3, approximately 15 pmol of a peptide corresponding to Val^{279}–Arg^{291}; peak 4, no sequence detected; peak 5, approximately 35 pmol of A^{266}GHPFMWNEHLGYVLTCPSNLGTGLR^{291} (Table 1). The peptide isolated in peak 3 is a chymotryptic-like fragment of the peptide isolated in peak 5 and was observed even though modified trypsin was used. The trypsin-generated peptide Ala^{266}–Arg^{291}, isolated in peak 5, overlaps and includes the

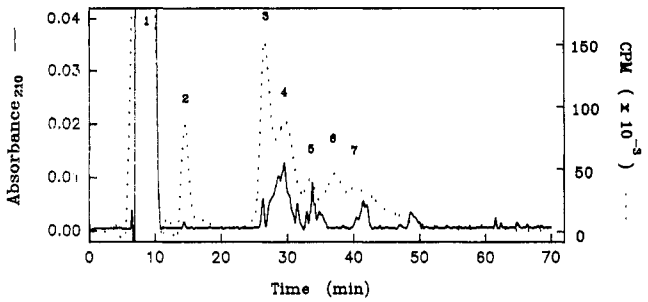

FIGURE 9: Reverse phase HPLC of immobilized Al^{3+}-purified tryptic peptides of heart creatine kinase photolabeled with [γ-^{32}P]2N_3ATP. 500 μg of rabbit heart creatine kinase was photolabled with 10 μM [γ-^{32}P]2N_3ATP and digested with modified trypsin as described under Materials and Methods. After purification by immoblized Al^{3+} affinity chromatography, the photolabeled peptides were injected into a reverse phase C8 column and eluted as described under Materials and Methods.

Table 2: Amino Acid Sequence Analysis of Radiolabeled Peptides from Rabbit Creatine Kinase Photolabeled with [γ-^{32}P]2N_3ATP and Digested with Trypsin

amino acid (pmol)	
heart	brain
V (118)	V (34)
I (92)	I (31)
S (47)	S (7)
M (49)	M (4)
E (55)	Q (17)
K (28)	K (14)

chymotrypsin-generated peptide detected in peak 3 from Figure 7B.

Photolabeled peptides from a tryptic digest of rabbit heart creatine kinase photolabeled with [γ-^{32}P]2N_3ATP were purified by immobilized Al^{3+} affinity chromatography. HPLC of these peptides gave the profile shown in Figure 9. Radioactive peaks 1 and 2 again contained no detectable peptide. Amino acid sequence analysis of peak 3 (retention time of 27 min) identified more than 100 pmol of the peptide V^{236}ISMEK (Table 2). More than 1.5×10^5 cpm was detected in this fraction. Analysis of peak 4 (retention time of 30 min) in Figure 9 yielded approximately 6 pmol of the peptide Val^{279}–Arg^{291}. No sequence was detected in peak 5 whereas no analysis was performed on peak 6 because of the lack of a corresponding absorbance. Analysis of peak 7 revealed the presence of 25 pmol of the peptide Ala^{266}–Arg^{291}.

To confirm the localization of the peptides Val^{236}–Lys^{241} and Val^{279}–Arg^{291} at the active site of creatine kinase, studies were done to determine if the same peptides within the BB isoform of rabbit creatine kinase were modified by photoaffinity labeling with [γ-^{32}P]2N_3ATP and [γ-^{32}P]8N_3ATP. HPLC of immobilized Al^{3+}-purified chymotryptic peptides from the BB isoform photolabeled with [γ-^{32}P]8N_3ATP revealed one major radioactive peptide peak (retention time of 30 min). Sequence analysis identified this peptide as I^{279}-LTCPSNLGTGLR^{291}, which corresponds to the homologous peptide in the MM isoform (Table 1). Immobilized Al^{3+} affinity chromatography, HPLC, and amino acid sequence analysis of tryptic peptides from the BB isoform photolabeled with [γ-^{32}P]2N_3ATP identified more than 30 pmol of VISMQK (Table 2) in the major radioactive peak (data not shown). No other peptides were detected. Like the major photolabeled peptide in Figure 9, this peptide also had a retention time of 27 min. As shown in Figure 10, V^{236}ISMQK corresponds to the homologous peptide in the M subunit of rabbit creatine kinase as identified above (V^{236}ISMEK).

```
                  220        230        240        250        260
Rabbit M : RGIWHNDNKSFLVWVNEEDHLRVISMEKGGNMKEVFRRFCVGLQKIEE
Rabbit B : R--------T----I----------Q---------T---N--TQ--T
Dog M    : R--------T----------Q----------
Rat M    : R----------------------------------------------
Chicken M : R--------T-----------------------------------K----
Torpedo C. M : R-----ND-----------------Q----------------K----
Rat B    : R--------T----I----------Q---------T---T--TQ--T
Human M  : P----------------------------------------------

                  270        280        290        300
Rabbit M : IFKKAGHPFMWNEHLGYVLTCPSNLGTGLRGGVHVKLAHLSKHPKFEE
Rabbit B : L--SKNYE----P----I----------A---I--P--GQ-E--SE
Dog M    : ----------------------------------------------E
Rat M    : ----------------------------------------N--------E
Chicken M : ----------T-----I-----------------PK--Q-----E
Torpedo C. M : --V---RG-------------------------IP--C--E--SE
Rat B    : L--SKNYE----P----I----------A---I--P--G--E--SE
Human M  : ----------Q----------------------------------E
```

FIGURE 10: Regions within cytosolic creatine kinase proposed to contain residues involved in the binding of the adenine moiety of ATP. Amino acid residues 214–309 from the primary sequence of the M and B subunits of rabbit and rat as well as the M subunit from four other species are shown. A dash indicates identity to the rabbit M subunit. Amino acids in boldface type reside in peptide regions photolabeled by azido analogs of ATP. Sequence data are from Perryman et al. (1986).

DISCUSSION

The results in this paper validate the specific interactions of 2N_3ATP and 8N_3ATP with the active sites of the MM and BB isoforms of creatine kinase. First, using two different techniques, we demonstrated that both 2N_3ATP and 8N_3-ATP could serve as substrates for the phosphoryl transfer reaction. Second, photolabeling with either analog caused a significant inhibition of enzymatic activity. Third, the natural substrate ATP was very effective at decreasing photoinsertion of these probes. Fourth, saturation of photoinsertion was observed when creatine kinase was photolabeled with either [γ-^{32}P]2N_3ATP or [γ-^{32}P]8N_3ATP. The cause of the decrease in photolabeling at concentrations of [γ-^{32}P]2N_3ATP above 15 μM in the saturation curve of Figure 5 is unclear. However, it was not caused by enzymatic turnover since the same curve was observed in the absence of creatine and since less than 1% of either analog was converted to creatine phosphate after 90 s of incubation of 4 °C. The determination of UV spectral properties during the course of the experiment ruled out tetrazole formation as a cause. The data from the control samples in the enzyme inhibition studies suggest that this anomaly may be the result of some type of interaction of the photoinduced product of 2N_3ATP with creatine kinase. The photoproduct, at higher concentrations, might interact with the active site with high enough affinity that it competes with and decreases the photoinsertion of intact 2N_3ATP.

Initial attempts to isolate photolabeled peptides of creatine kinase using Fe^{3+} as the immobilized metal were complicated by the retention of carboxylic acid-rich peptides. Apparently, negatively charged glutamate and aspartate residues, when occurring in clusters, can provide a strong enough coordination with the immobilized Fe^{3+} that they are retained on the column along with the photolabeled peptides. Also, it has been shown by others that surface histidyl groups of selected thiol-free model proteins bind to immobilized Fe^{3+} (Hemdan et al., 1989). Thus, depending on the primary structure of a protein (e.g., clusters of negatively charged residues or histidyl groups), Fe^{3+} may not always be the metal of choice for the purification of phosphate-containing peptides by immobilized metal affinity chromatography.

The results from Figure 8 and the subsequent amino acid analysis demonstrated that immobilized Al^{3+} was more selective for the triphosphate group than immobilized Fe^{3+} since neither of the carboxylic acid-rich peptides was detected. In fact, only two peptides (Ala^{266}–Arg^{291} and Val^{279}–Arg^{291}) were present in sufficient quantity to be sequenced. Thus,

very few peptides were retained on the immobilized Al^{3+} column. Since every one of the peptides detected in Figures 7B, 8, and 9 corresponded to a major radioactive peak, it appears as if only the photolabeled peptides were significantly retained by the immobilized Al^{3+} column. The other small A_{210} peaks observed in these figures may represent minor levels of nonphotolabeled peptides retained by the Al^{3+} column or may represent UV-absorbing material from the Sepharose resin.

The efficiency of the immobilized Al^{3+} column is illustrated in Figure 7 when one compares the number and amount of peptides in the flow-through (panel A) and eluate (panel B) from the column. The photolabeled peptide (and only peptide) observed in panel B had an absorbance of about 0.02. whereas many of the flow-through peptides in panel A had a combined absorbance of greater than 1. Comparing the differences in radioactivity associated with the peptides, less than 5×10^3 cpm was associated with the flow-through peptides, whereas more than 1.8×10^6 cpm was present in the fraction containing the single peptide detected in the eluate. Thus, immobilized Al^{3+} affinity chromatography is a very effective technique for the separation of photolabeled peptides from nonmodified peptides.

A major problem encountered during HPLC of both direct and photoaffinity-labeled peptides is the loss of ^{32}P-radiolabel. Apparently, the inherent lability of the N-glycosidic bond within the photoinserted nucleotide and/or the covalent bond formed between the protein and nucleotide upon photolysis renders the radiolabel vulnerable to loss during reverse phase HPLC. Decreasing the flow rate sometimes improves the retention of radiolabel (unpublished results). Results from the metal ion studies using photolabeled peptides of creatine kinase and 3-phosphoglycerate kinase indicate that inclusion of Al^{3+} in HPLC solvents also enhances the retention of radiolabel during HPLC of photolabeled peptides.

Immobilized Al^{3+} affinity chromatography, HPLC, and sequence analysis of peptides from creatine kinase photolabeled with [γ-^{32}P]8N_3ATP revealed that the peptide region 279–291 is localized within the adenine-binding domain of creatine kinase. Evidence for the involvement of this region is as follows: (1) This sequence was found in the peptides isolated and identified from both the chymotryptic and tryptic digests of the photolabeled MM isoform. (2) The corresponding region was photolabeled in the BB isoform. (3) The same region was also photolabeled by [γ-^{32}P]2N_3ATP.

The observation that [γ-^{32}P]2N_3ATP photoinserts into more than one peptide is not that unusual since previous studies with adenylate kinase (Salvucci et al., 1992) and other proteins have shown that a given photoprobe may photoinsert into more than one amino acid during a single photolabeling experiment. If two different amino acid residues are in close proximity to the azido group at the time of photolysis, photoinsertion may occur at either residue. If these two residues reside within different proteolytic fragments, then more than one peptide will become modified. The ratio of photolabeling these two peptides is likely dependent on the freedom of rotation of the base and the syn/anti ratio of the nucleotide photoprobe.

In summary, we have used immobilized Al^{3+} affinity chromatography and reverse phase HPLC to isolate and identify the peptides within the MM and BB isoforms of rabbit creatine kinase that were photolabeled by [γ-^{32}P]2N_3ATP and [γ-^{32}P]8N_3ATP. The observation that the primary site of photoinsertion of these two probes was into two different peptides demonstrates the utility of using the 2-azido and 8-azido analogs of ATP to potentially identify distinct regions within the adenine-binding domain of ATP-binding proteins. We conclude that amino acid residues within the peptide regions 236–241 and 279–291 of rabbit cytosolic creatine kinase comprise part of the binding domain for the adenine moiety of ATP. These data suggest that these two regions within the primary sequence are in close proximity in the three-dimensional structure of cytosolic creatine kinase. This information should prove to be useful in the design of future mutagenesis studies that investigate the involvement of specific amino acid residues in substrate-binding and/or catalysis. Finally, we have described two technical advances which should have broad applications in other studies involving the isolation and identification of photoaffinity-labeled peptides.

ACKNOWLEDGMENT

We thank Dr. Cristopher Mathews and Dr. Britt-Marie Sjöberg for their critique of the manuscript.

REFERENCES

Andersson, L., & Porath, J. (1986) *Anal. Biochem. 154*, 250–254.
Bessman, S. P., & Carpenter, C. L. (1985) *Annu. Rev. Biochem. 54*, 831–862.
Borders, C. L., Jr., & Riordan, J. F. (1975) *Biochemistry 14*, 4699–4704.
Buechter, D. D., Medzihradsky, K. F., Burlingame, A. L., & Kenyon, G. L. (1992) *J. Biol. Chem. 267*, 2173–2178.
Chavan, A. J., Nemoto, Y., Narumiya, S., Kozaki, S., & Haley, B. E. (1992) *J. Biol. Chem. 267*, 14866–14870.
Chavan, A. J., Ensor, C. M., Wu, P., Haley, B. E., & Tai, H. H. (1993) *J. Biol. Chem. 268*, 16437–16442.
Clarke, D. E., & Price, N. C. (1979) *Biochem. J. 181*, 467–475.
Furter, R., Furter-Graves, E. M., & Wallimann, T. (1993) *Biochemistry 32*, 7022–7029.
Harrison, T. R. (1991) in *Principles of Internal Medicine* (Wilson, J. O., et al., Eds.) pp 953, 2091, McGraw-Hill, Inc., Philadelphia, PA.
Hemdan, E. S., Zhao, Y., Sulkowski, E., & Porath, J. (1989) *Proc. Natl. Acad. Sci. U.S.A. 86*, 1811–1815.
James. T. L., & Cohn, M. (1974) *J. Biol. Chem. 249*, 2599–2604.
Kim, H., & Haley, B. E. (1990) *J. Biol. Chem. 265*, 3636–3641.
Laemmli, U. K. (1970) *Nature 227*, 680–685.
Mahowald, T. A. (1965) *Biochemistry 4*, 732–740.
Mahowald, T. A., Noltmann, E. A., & Kuby, S. A. (1962) *J. Biol. Chem. 237*, 1535–1548.
Marletta, M. A., & Kenyon, G. L. (1979) *J. Biol. Chem. 254*, 1879–1886.
Michelson, A. M. (1964) *Biochim. Biophys. Acta* **91**, 1–13.
Murakami, N., Healy-Louie, G., & Elzinga, M. (1990) *J. Biol. Chem. 265*, 1041–1047.
Muszynska, G., Andersson, L., & Porath, J. (1986) *Biochemistry 25*, 6850–6853.
Olcott, M. C., & Haley, B. E. (1993) *FASEB J. 7*, A838.
O'Sullivan, W. J., & Cohn, M. (1966) *J. Biol. Chem. 241*, 3116–3125.
Perryman, M. B., Kerner, S. A., Bohlmeyer, T. J., & Roberts, R. (1986) *Biochem. Biophys. Res. Commun. 140*, 981–989.
Potter, R. L., & Haley, B. E. (1993) *Methods Enzymol. 91*, 613–633.
Rosevear, P. R., Desmeules, P., Kenyon, G., & Mildran, A. S. (1981) *Biochemistry 21*, 6155–6164.
Salvucci, M. E., Chavan, A. J., & Haley, B. E. (1992) *Biochemistry 31*, 4479–4487.
Shoemaker, M., & Haley, B. E. (1993) *Biochemistry 32*, 1883–1890.
Turner, D. C., Wallimann, T., & Eppenberger, H. M. (1973) *Proc. Natl. Acad. Sci. U.S.A. 70*, 702–705.
Walliman, T., Turner, D. C., & Eppenberger, H. M. (1977) *J. Cell Biol. 75*, 297–317.